

Supplementary Information (SI)

Unveiling different physicochemical properties of M-doped β -NaFeO₂ (where M = Ni or Cu) materials evaluated as CO₂ sorbents: A combined experimental and theoretical analysis

Nayeli Gómez-Garduño^a, Daniel G. Araiza^{a,b,*}, Christian A. Celaya^{c,d,*}, Jesús Muñiz^c,
Heriberto Pfeiffer^a

^aInstituto de Investigaciones en Materiales, Universidad Nacional Autónoma de México,
Circuito Exterior s/n, Ciudad Universitaria, Del. Coyoacán, C.P. 04510, Ciudad de México,
Mexico

^bPresent address: Instituto de Ciencias Aplicadas y Tecnología, Universidad Nacional
Autónoma de México, Ciudad de México, C.P. 04510, Mexico

^cInstituto de Energías Renovables, Universidad Nacional Autónoma de México, Priv.
Xochicalco s/n, Col. Centro, Temixco, C.P. 62580, Morelos, Mexico

^d Present address: Centro de Nanociencias y Nanotecnología, Universidad Nacional
Autónoma de México, Km 107 Carretera Tijuana-Ensenada, Ensenada, B.C., C.P. 22800,
Mexico.

*Corresponding author: araiza@materiales.unam.mx (D.G. Araiza) and
acelaya@ier.unam.mx (C.A. Celaya)

S.1 Characterization of materials

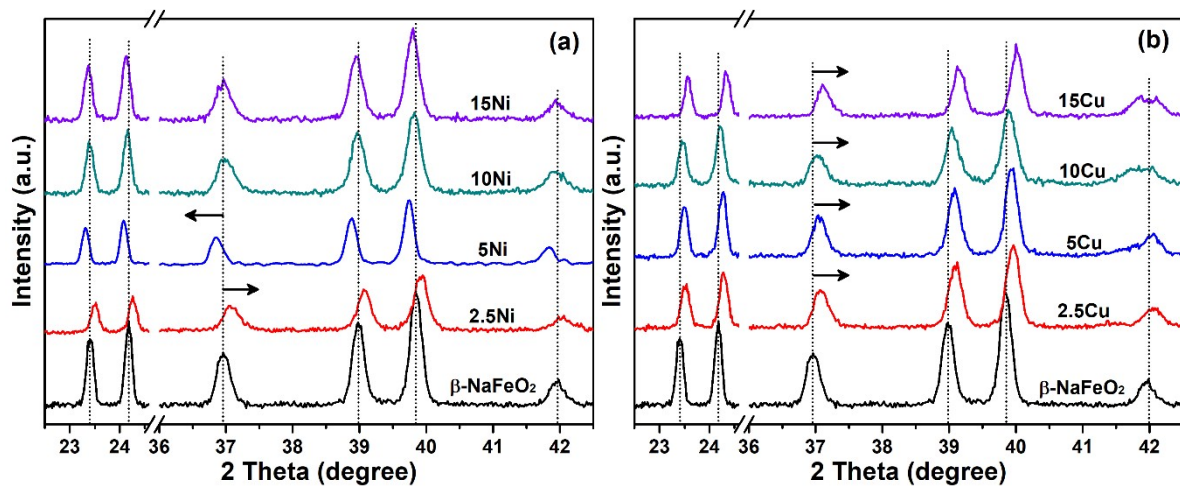


Fig. S1. Amplification of the XRD patterns, showing the most intense peaks coming from the $\beta\text{-NaFeO}_2$ phase for each sample series: (a) $X\text{Ni}-\text{NaFeO}_2$ and (b) $X\text{Cu}-\text{NaFeO}_2$.

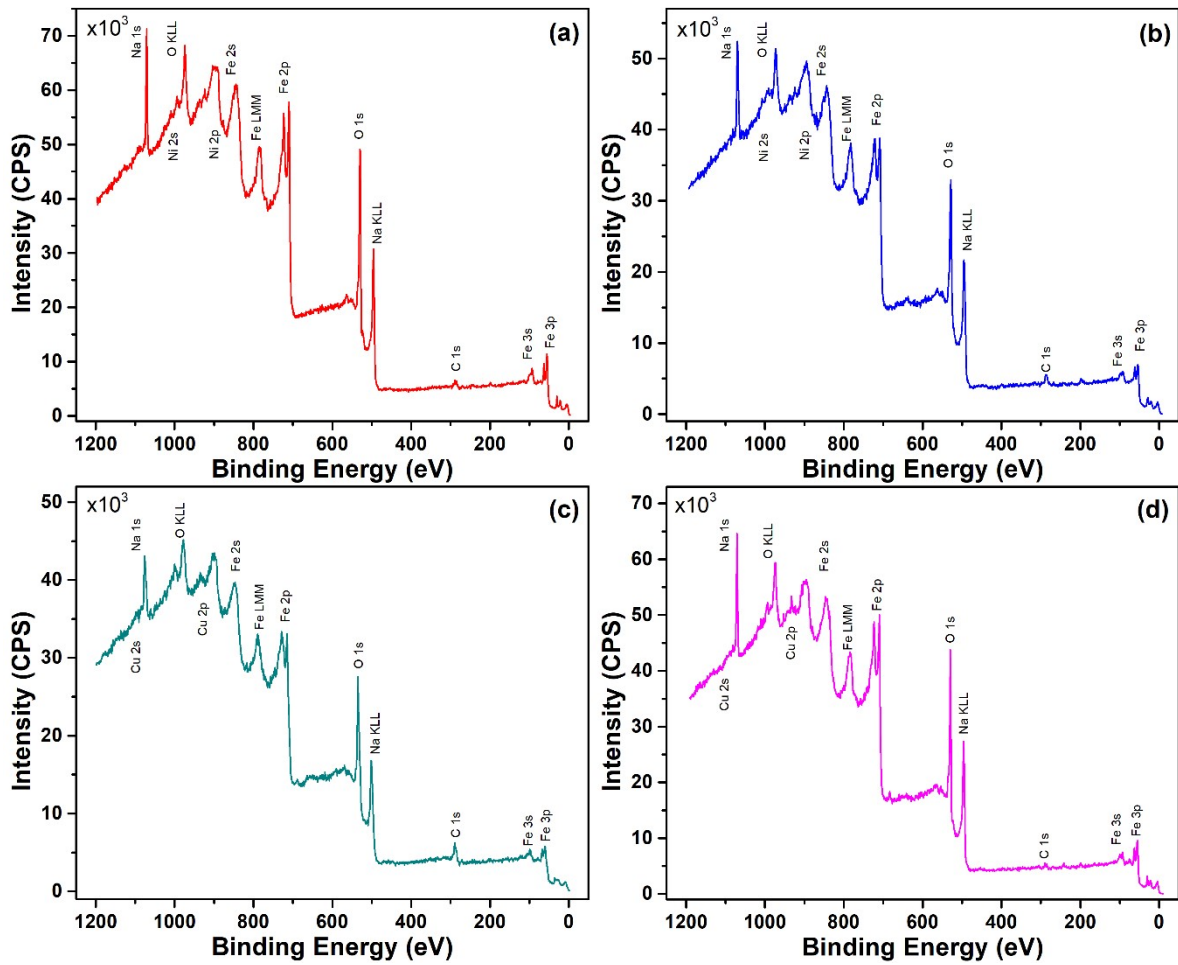


Fig. S2. XPS survey spectra of: (a) 2.5Ni-NaFeO₂, (b) 5Ni-NaFeO₂, (c) 2.5Cu-NaFeO₂ and (b) 5Cu-NaFeO₂ samples.

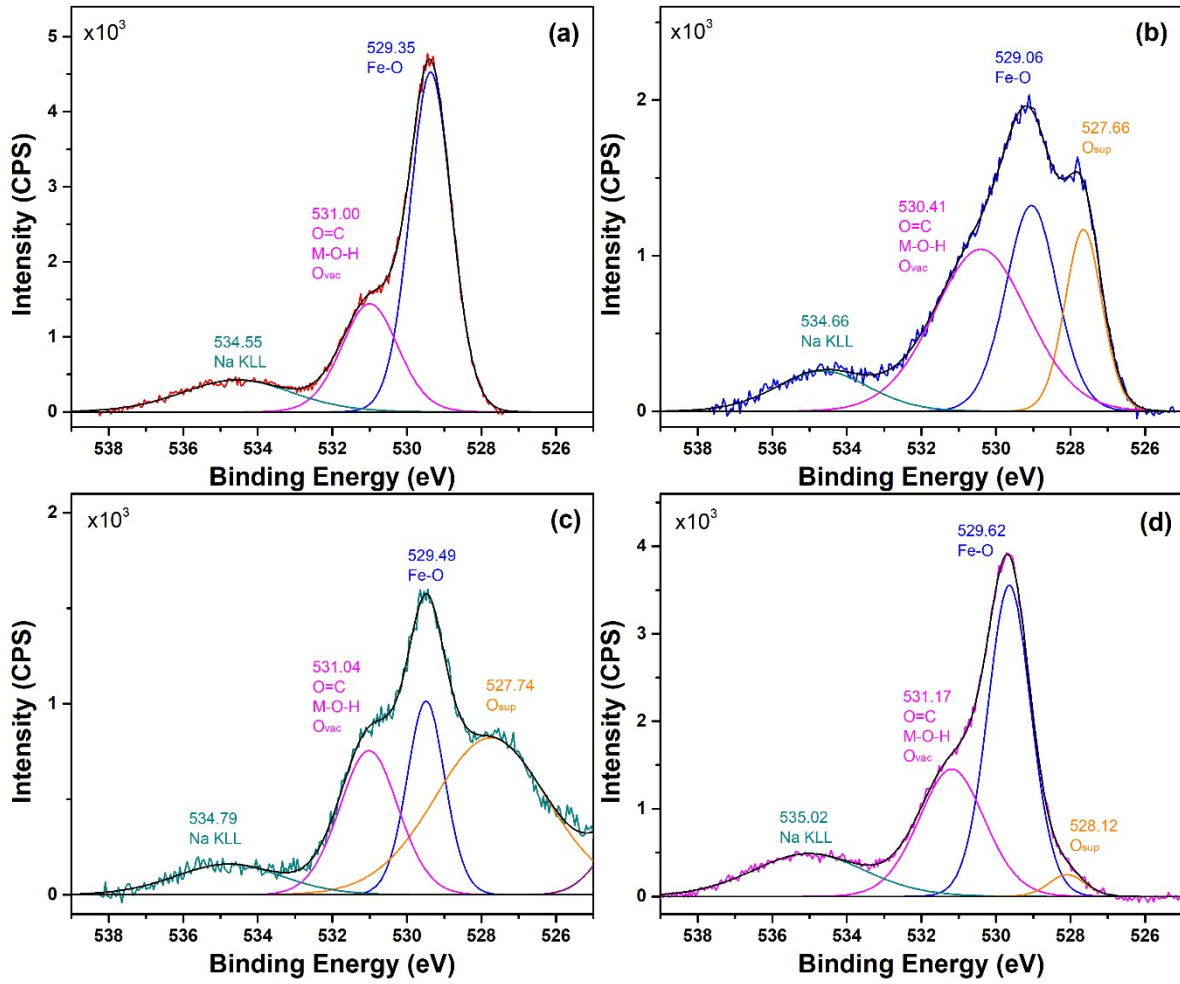


Fig. S3. High resolution XPS spectra of the O 1s edge: (a) 2.5Ni-NaFeO₂, (b) 5Ni-NaFeO₂, (c) 2.5Cu-NaFeO₂ and (d) 5Cu-NaFeO₂ samples.

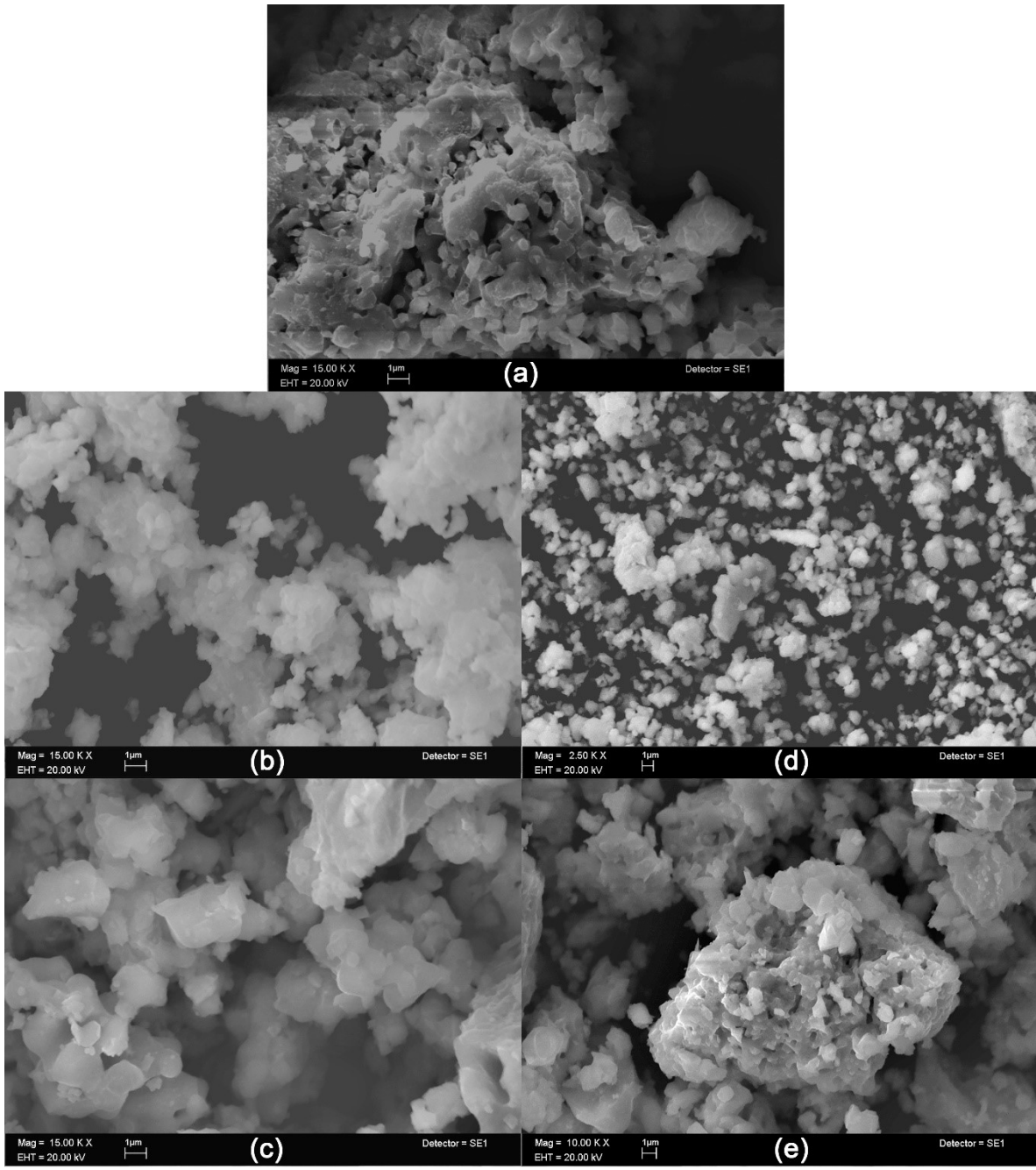


Fig. S4. Representative secondary electron images of selected $XM\text{-NaFeO}_2$ doped ferrites: (a) Pristine β -NaFeO₂, (b) 5Ni-NaFeO₂, (c) 5Cu-NaFeO₂, (d) 2.5Ni-NaFeO₂ and (e) 2.5Cu-NaFeO₂.

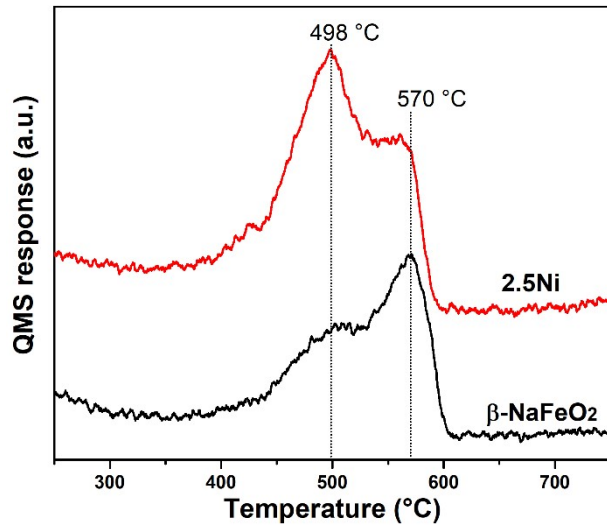


Fig. S5. CO₂-TPD desorption profiles for the pristine β-NaFeO₂ and 2.5Ni-NaFeO₂ samples thermally treated from 200 to 800 °C in a N₂ flow.

S.2 DFT calculations

Table S1. Cell parameter values (Å) of the fully relaxed orthorhombic β-NaFeO₂ structure. The lattice parameters are labeled as **a**, **b**, and **c**.

Axis	Cell parameter values (Å)		
	Calculated – DFT+U	Experimental – Rietveld	Reference [75]
<i>a</i>	5.779	5.668	5.682
<i>b</i>	5.419	5.384	5.425
<i>c</i>	7.155	7.146	7.235

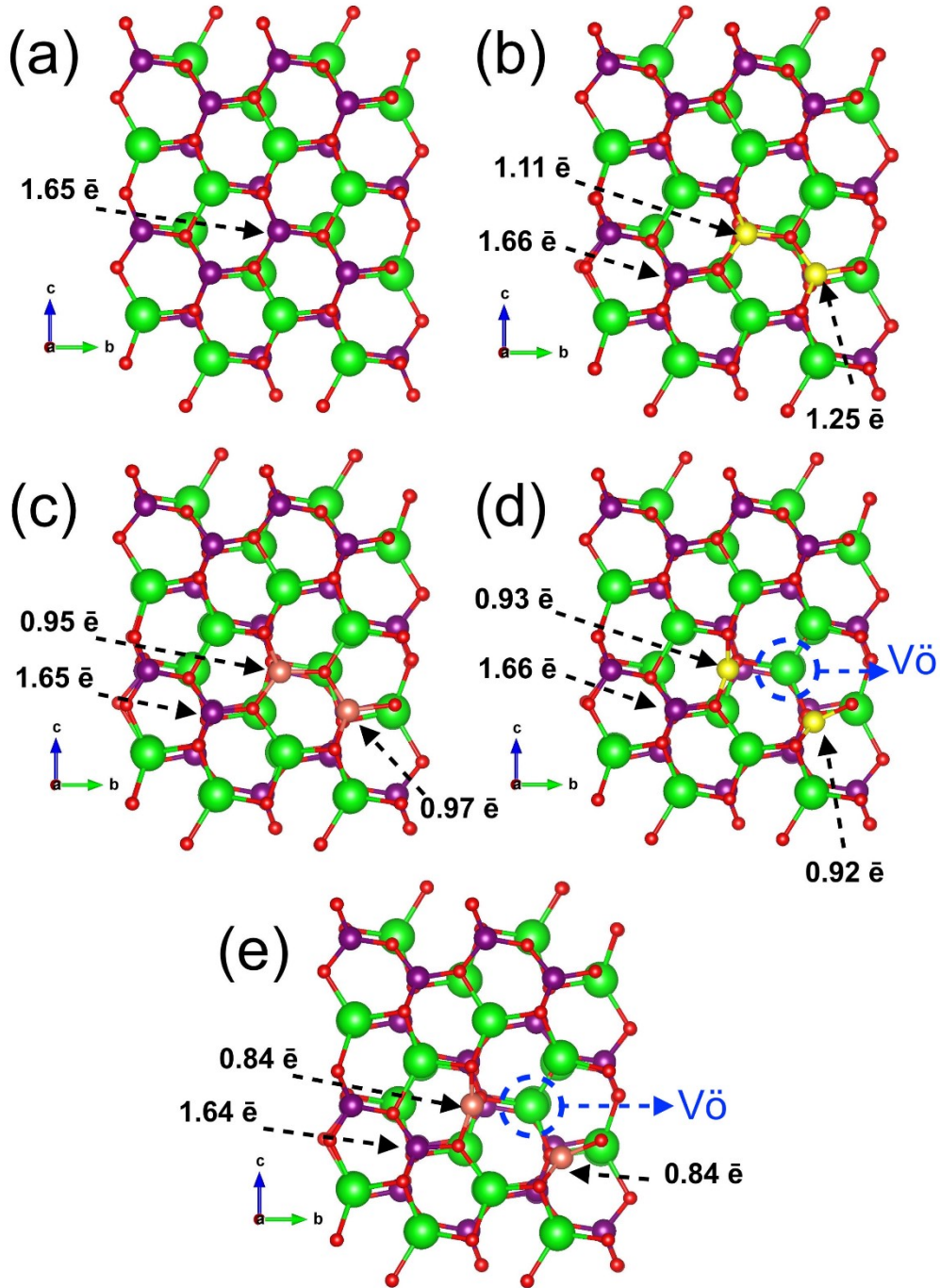


Fig. S6. Relaxed atomic geometries for: (a) pristine β -NaFeO₂, (b) Ni-NaFeO₂, (c) Cu-NaFeO₂, (d) Ni-NaFeO₂-Vö, and (e) Cu-NaFeO₂-Vö structures. Colour code: Na (Green), O (Red), Fe (Purple), Ni (Yellow), and Cu (Bronze). The site of oxygen vacancy is denoted by the blue dotted circle. The text and black arrows indicate the Bader charge population computed by DFT+U method.

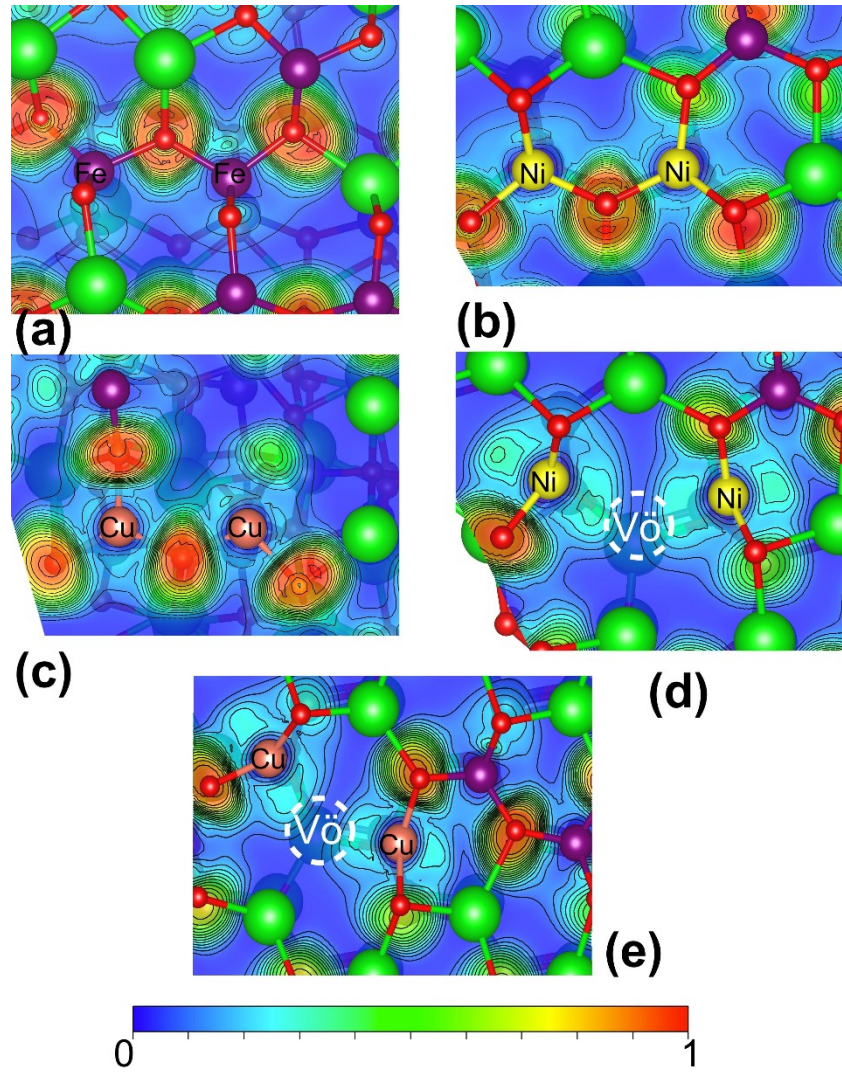


Fig. S7. 2D slice of the electronic localization function (ELF) for: (a) pristine β -NaFeO₂, (b) Ni-NaFeO₂, (c) Cu-NaFeO₂, (d) Ni-NaFeO₂-Vö, and (e) Cu-NaFeO₂-Vö structures. Colour code: Na (Green), O (Red), Fe (Purple), Ni (Yellow), and Cu (Bronze). The oxygen vacancy site is denoted by the blue dotted circle.

Table S2. Geometrical parameters (\AA) of the fully relaxed pristine and M-doped ferrites. Values were calculated at the spin-polarized GGA-PBE level of theory.

Bond type	Bond length (\AA)				
	$\beta\text{-NaFeO}_2$	Ni-NaFeO_2	Cu-NaFeO_2	$\text{Ni-NaFeO}_2\text{-V}\ddot{\text{o}}$	$\text{Cu-NaFeO}_2\text{-V}\ddot{\text{o}}$
Na–O	2.473	2.437	2.470	2.428	2.297
Fe–O	1.840	1.836	1.838	1.838	1.814
Na–Fe	3.283	3.494	3.285	3.294	3.512
M–O ^a	n/a	1.929	2.001	1.865	1.922

^aM is associated with Ni or Cu

Table S3. Theoretical (Theo.) and experimental (Exp.) band gap energy (E_{gap}) values, band gap difference (ΔE_{gap}), relative error (E_{error}), and magnetization moment (μ_B) of the pristine and M-doped ferrites, calculated at the spin-polarized GGA-PBE level of theory.

System	E_{gap} (eV)		ΔE_{gap} (eV)	E_{error} (%)	Magnetization moment (μ_B)
	Theo.	Exp.			
$\beta\text{-NaFeO}_2$	1.87	1.80	0.07	3.88	n/a
Cu-NaFeO_2	1.90	1.76-1.78	0.13	7.34	-0.57
Ni-NaFeO_2	1.97	1.82-1.81	0.16	8.83	-0.13
$\text{Cu-NaFeO}_2\text{-V}\ddot{\text{o}}$	1.76	1.76-1.78	0.01	0.56	-0.48
$\text{Ni-NaFeO}_2\text{-V}\ddot{\text{o}}$	1.85	1.82-1.81	0.04	2.20	-1.53

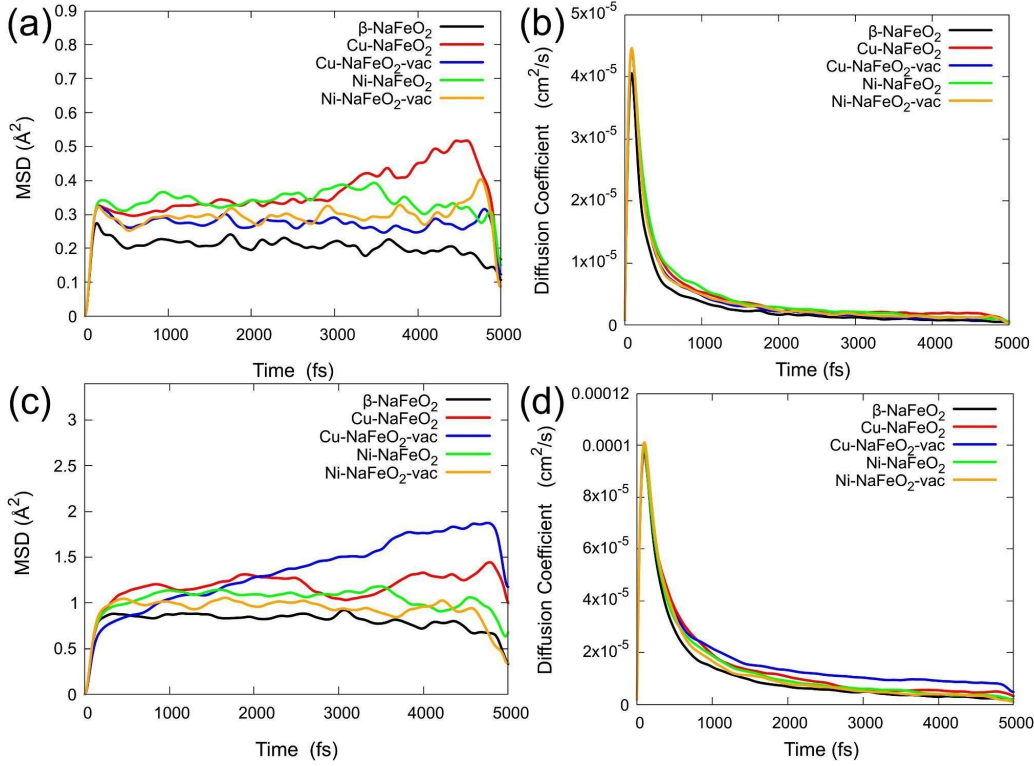


Fig. S8. Mean square displacements (MSD), and diffusion coefficient of Na in sodium ferrite systems at (a-b) a temperature of $T = 200\text{ }^{\circ}\text{C}$, and (c-d) $T = 800\text{ }^{\circ}\text{C}$. The Na diffusion coefficient was

$$D_{\text{Na}} = \frac{1}{6t} \left[\sum_i |\Delta r_i(t)|^2 \right]$$

obtained according to

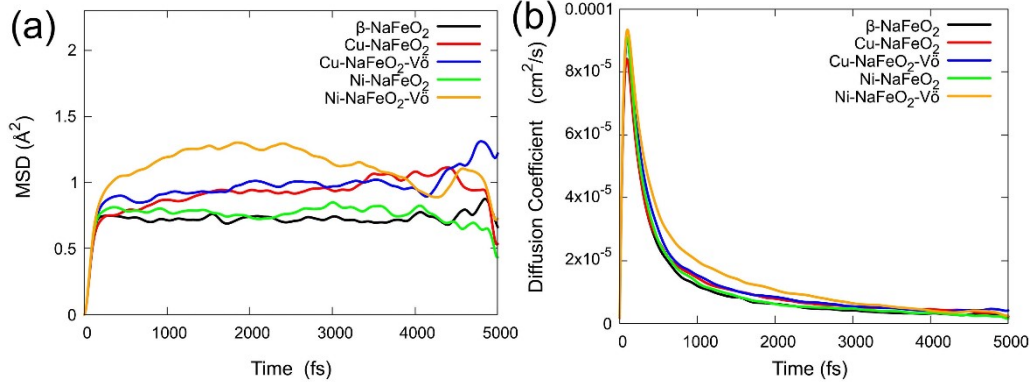


Fig. S9. (a) Mean square displacements (MSD), and (b) Na diffusion coefficient in the sodium ferrite systems at $T = 700\text{ }^{\circ}\text{C}$.

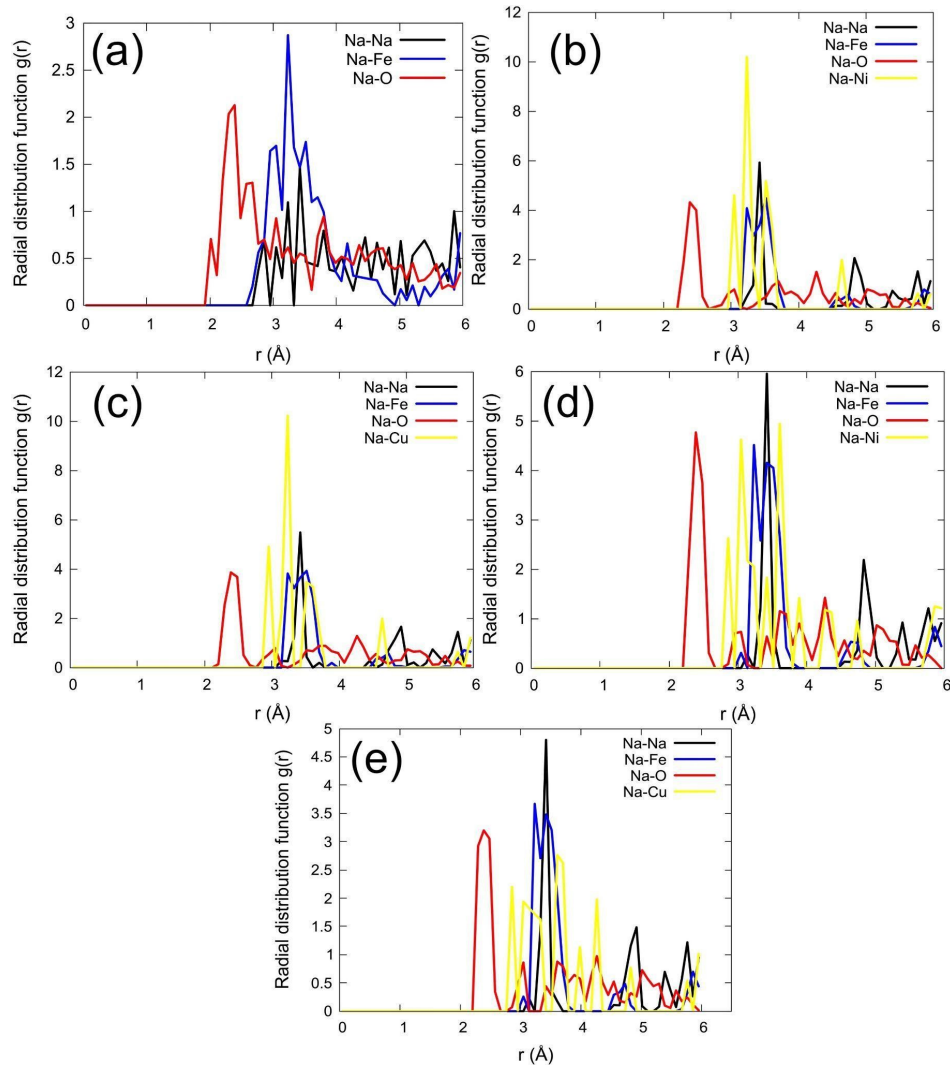


Fig. S10. Radial distribution functions (RDF) at a temperature of $T = 200$ °C obtained with the AIMD simulations: (a) pristine β -NaFeO₂, (b) Ni-NaFeO₂, (c) Cu-NaFeO₂, (d) Ni-NaFeO₂-Vö, and (e) Cu-NaFeO₂-Vö structures.

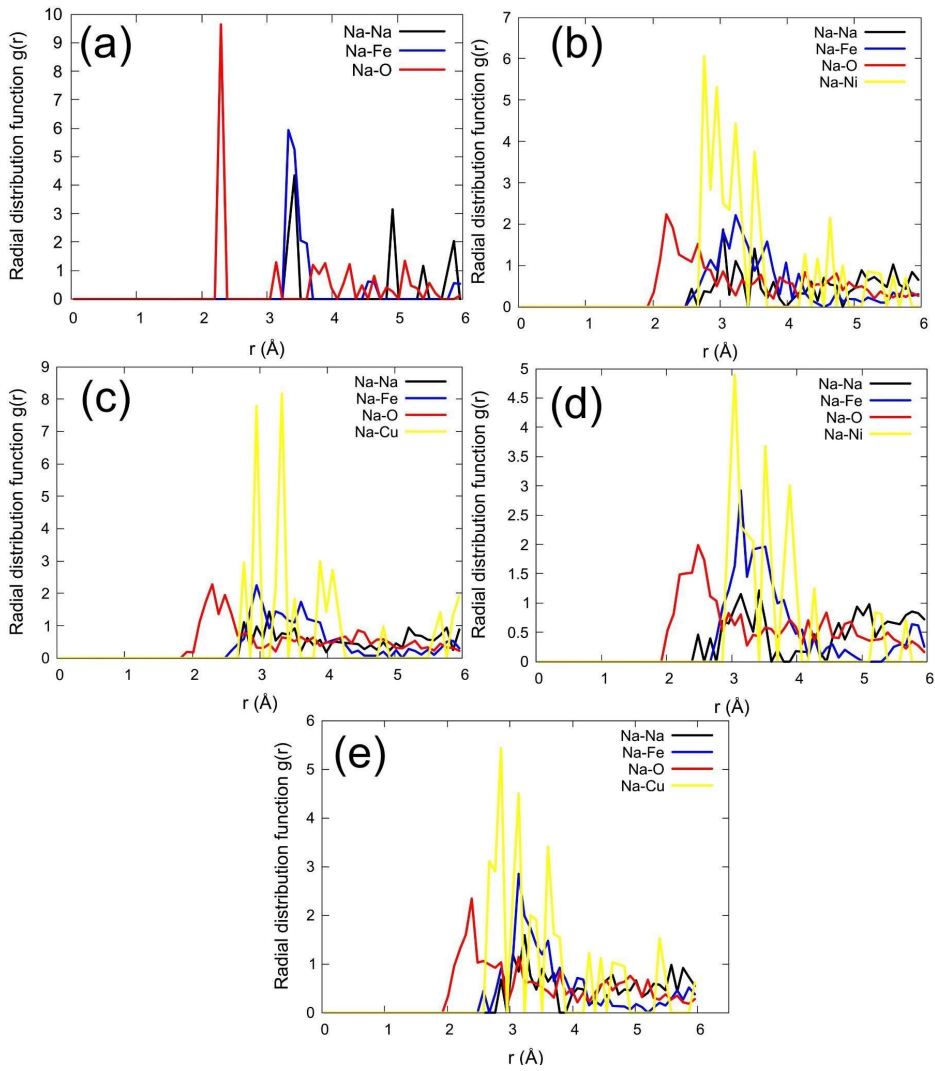


Fig. S11. Radial distribution functions (RDF) at a temperature of $T = 800 \text{ } ^\circ\text{C}$ obtained with the AIMD simulations: (a) pristine $\beta\text{-NaFeO}_2$, (b) Ni-NaFeO_2 , (c) Cu-NaFeO_2 , (d) $\text{Ni-NaFeO}_2\text{-V}\ddot{\text{o}}$, and (e) $\text{Cu-NaFeO}_2\text{-V}\ddot{\text{o}}$ structures.

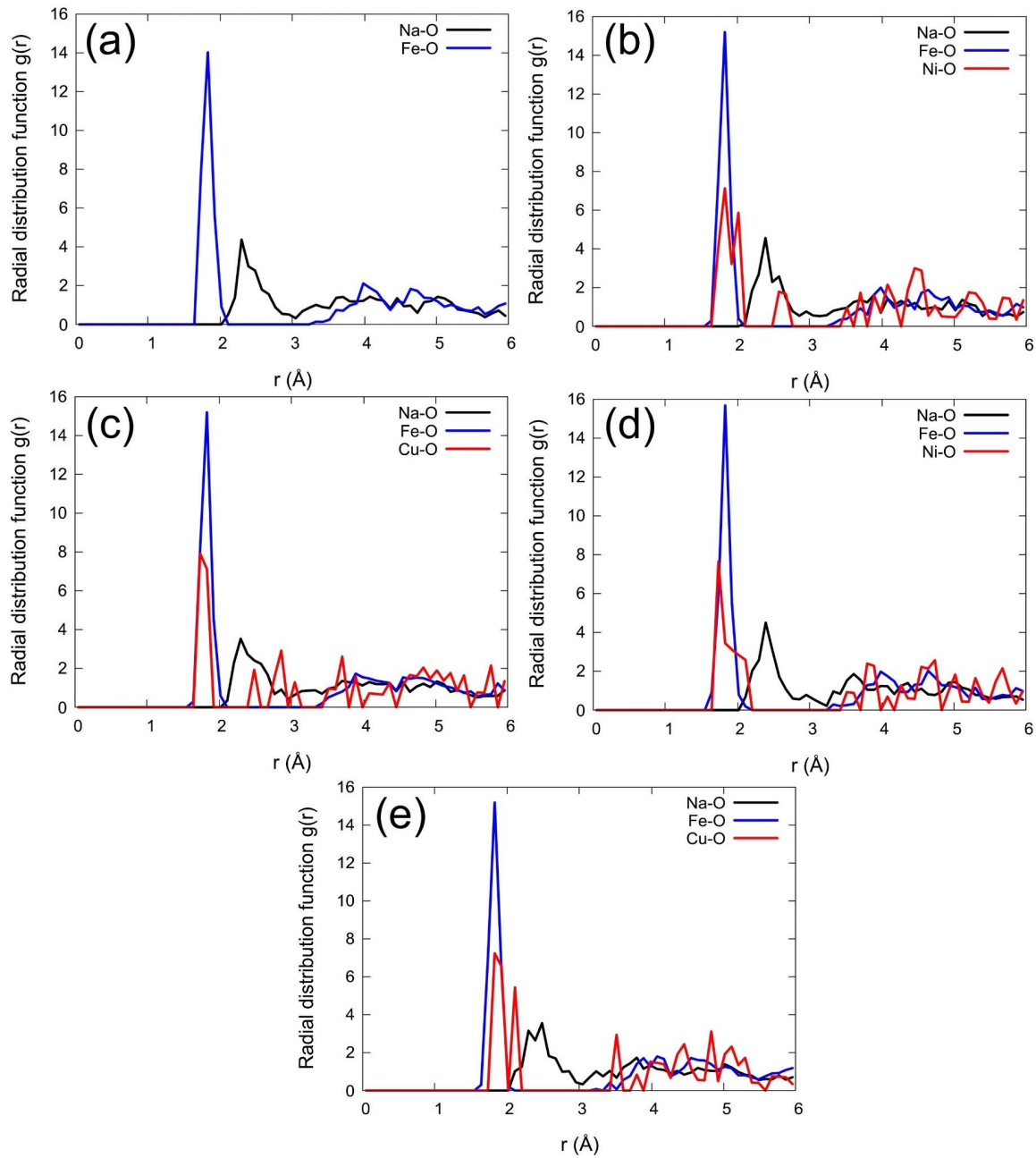


Fig. S12. Radial distribution functions (RDF) for oxygen interaction at a temperature of $T = 200$ °C obtained with the AIMD simulations: (a) pristine $\beta\text{-NaFeO}_2$, (b) Ni-NaFeO₂, (c) Cu-NaFeO₂, (d) Ni-NaFeO₂-Vö, and (e) Cu-NaFeO₂-Vö structures.

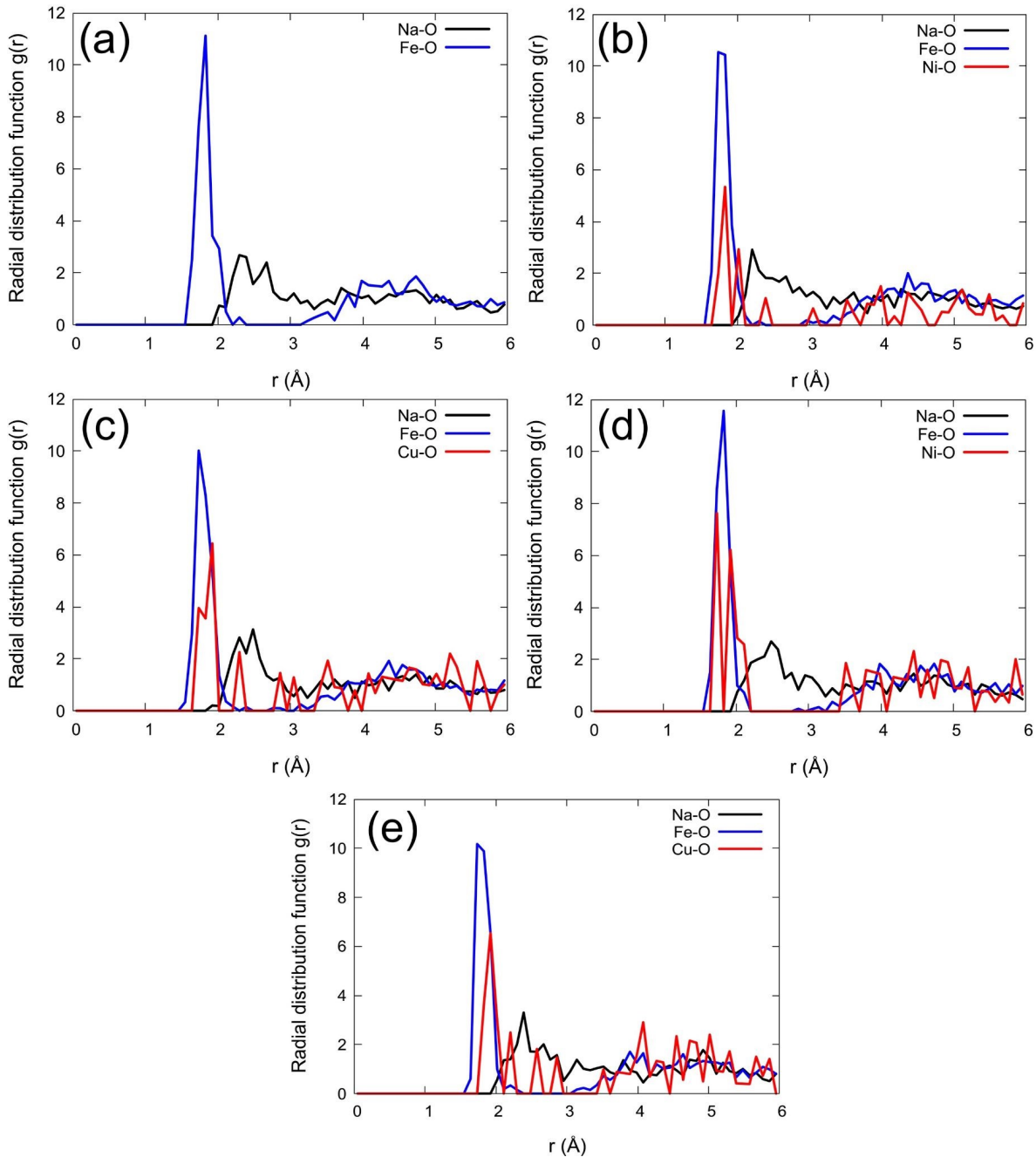


Fig. S13. Radial distribution functions (RDF) for oxygen interaction at a temperature of $T = 800$ °C obtained with the AIMD simulations: (a) pristine $\beta\text{-NaFeO}_2$, (b) Ni-NaFeO₂, (c) Cu-NaFeO₂, (d) Ni-NaFeO₂-Vö, and (e) Cu-NaFeO₂-Vö structures.